

---

**MODELS FOR THE DESCRIPTION  
OF ALLOY FORMATION WITH NONEQUILIBRIUM  
COMPOSITION IN THE DIFFUSION CONTACT REGION  
BETWEEN TWO COMPONENTS UNDER PULSE LOADING****A.O. KOVAL'CHUK, D.S. GERTSRIKEN, A.M. GUSAK, V.F. MAZANKO,  
N.V. TYUTYUNNYK, O.I. MALIY**UDC 548.526  
© 2009**B. Khmelnytskyi Cherkasy National University**  
(81, Shevchenko Blvd., Cherkasy 18000, Ukraine; e-mail: akov@cdu.edu.ua)

---

Formation of metastable alloys, the solubility limits of which are much higher than the corresponding equilibrium values and depend on the deformation rate, are observed very often in experiments dealing with diffusion in metals and alloys under pulse loading. Three microscopic models based on the concept of "ballistic jumps", which was put forward by G. Martin *et al.* for metals under irradiation or ball-milling conditions, have been proposed to describe this process: (i) the exchange-diffusion model, (ii) the model of interstitial migration, and (iii) the vacancy model of diffusion. Dynamic phase diagrams have been calculated in the framework of all those models. A qualitative agreement between the theoretical results and available experimental data has been obtained.

---

**1. Experimental Part**

Our experimental researches of mass transfer under the action of pulse loading of diffusion couples with high deformation rates ( $\dot{\epsilon} \geq 1 \text{ s}^{-1}$ ) testify to anomalous penetration depths and to the formation of nonequilibrium solid solutions [1]. The experiments were carried out making use of cylindrical  $10 \times 10\text{-mm}^2$  specimens fabricated of annealed iron, nickel, or copper with the surface finish of contacting end surfaces not lower than  $\nabla 13$ . The features of atomic migration and phase formation at the interaction between different metals subjected to the shock compression were studied on an installation that was usually used for shock welding in vacuum (see Fig. 1) [2]. This installation allows a pulse loading to be realized with the help of a weight (of 1 to 50 kg) that falls down onto cylindrical specimens from a height of 2 to 6 m either under

the action of the terrestrial gravitation or due to an additional pneumatic push. The specimens were heated up preliminarily, and the initial distance between them was about 1 mm. To fix the phase composition of specimens, which was formed in the diffusion zone at the given temperature, the so-called electron guns were switched off at the moment, when the weight stroke the upper specimen; additionally, when the anvil was hit, i.e. in 1 to 10 ms, specimens were flooded with liquid nitrogen. The average deformation degree was 10–25%, and the deformation rate varied from 0.5 to  $300 \text{ s}^{-1}$ . The temperature increment due to a specimen deformation induced by the collision of specimens under the action of a falling weight did not exceed  $10 \text{ }^\circ\text{C}$  [3, 4].

The loading time was measured experimentally making use of a loop oscillograph, and it amounted to  $10^{-3} - 10^{-2} \text{ s}$ . Depending on the dimensions of the material and the cooling intensity, the time of cooling of specimens down to room temperature was equal to several seconds. The rate of plastic deformation was calculated by the formula  $\dot{\epsilon} = \frac{\Delta h/h_0}{\tau}$ , where  $\Delta h$  is a reduction of the specimen height, and  $h_0$  is the initial height.

When calculating the nonequilibrium state diagrams, we selected the concentrations that had been measured directly in the contact region between two specimens, i.e. the maximal values [5, 6]. To determine the content of a dissolved substance, we used the methods of X-ray diffraction analysis and X-ray microspectrometry.

The typical dynamic phase diagrams for Cu–Ni and Fe–Cu couples at various deformation rates are shown in Fig. 2 (the data were taken from work [1]). A characteristic width of regions with nonequilibrium composition was about one micron. A preliminary analysis [7,8] demonstrated that the vacancy mechanism cannot provide such a mixing after a very short loading. Probable alternatives include “mechanical” diffusion and migration of interstitial sites following the “kick-out” mechanism, if defects are generated rather quickly.

In this work, we consider only the problem of the formation of metastable solid solutions. The mechanisms of this phenomenon still remain obscured. Nowadays, there is no conventional theory describing it. In what follows, we discuss our models of nonequilibrium solution formation, which are based on the ideas proposed by Martin [9] for alloys subjected to irradiation.

## 2. Application of the Ballistic Jump Concept to Pulse Loading

In work [9], the concept of the so-called ballistic jumps was formulated for the first time and applied to alloys subjected to high-energy irradiation. The concept consists in that, when considering diffusion, an additional term  $b$  independent of the temperature and associated with the irradiation should be taken into account in the expression for the frequency of diffusion events  $\nu$ , along with the standard Arrhenius term  $\nu_0 \exp(-Q/kT)$  associated with thermal fluctuations:

$$\nu = \nu_0 \exp(-Q/kT) + b. \quad (1)$$

The so-called ballistic jumps, which take place when irradiating particles collide with crystal atoms, rather than the thermal ones are responsible for the appearance of the term  $b$ . A somewhat similar situation may be expected in the case of mechanical action on a specimen. From our viewpoint, an essential feature is that such a non-Arrhenius behavior should manifest itself in single-crystalline grains, because it is in these grains that supersaturated solid solutions are formed. In this connection, the character of a macroscopic deformation (plasticity/elasticity) can be not principal. To estimate the possibility of ballistic jump induction in a single crystal subjected to a pulse impact, we calculated the molecular dynamic behavior of a point defect, when a shock wave propagates through the specimen.

To simulate the process, we used the Born–Mayer potential  $\Phi(r) = A \exp[\alpha(1 - r/r_0)]$ , which provided the correct self-diffusion coefficients for copper at  $A = 0.05$

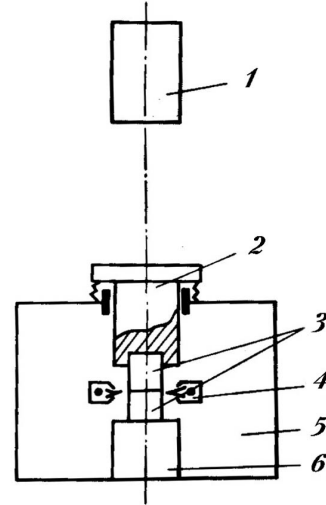


Fig. 1. Block scheme of installation: weight (1), striker (2), specimens (3), ring heaters (4), vacuum chamber (5), and anvil (6)

eV, the radius of the first coordination sphere for copper  $r_0 = 2.55 \text{ \AA}$ , and  $\alpha = 13.9$  [10].

Numerical calculations were carried out using an improved Euler scheme with the time step  $dt = 10^{-15} \text{ s}$ . An fcc single crystal of copper  $29 \times 29 \times 29$  interplane distances of the  $\{100\}$  family in dimension was selected for simulation. An interstitial atom was artificially introduced into the octahedral interstitial site of the crystal, and the initial state was made relaxed using the molecular statics method. The calculation of shock wave motion was carried out at zero temperature. The shock wave was generated by moving the first two atomic planes with a constant velocity  $v$ . The boundary conditions in this model were as follows: the coordinates of atoms belonging to two external atomic planes were considered fixed along the shock wave motion direction (direction (100)), and the periodic Born–von Karman boundary conditions were imposed along both axes perpendicular to the direction of shock wave propagation.

The number  $i$  of an atomic plane, for which the condition  $(v_i - \frac{v}{2})(v_{i-1} - \frac{v}{2}) < 0$  was satisfied, was selected as the wave front criterion. Here,  $v_i$  and  $v_{i-1}$  are the average projections of the velocities of the  $i$ -th and  $(i-1)$ -th atomic planes, respectively, onto the direction of shock wave propagation, and  $v$  is the impact velocity. At  $v = 200 \text{ m/s}$ , the point defect is captured by the wave front: a series of “kicks-out” is generated (in so doing, the defect is certainly represented by different interstitial

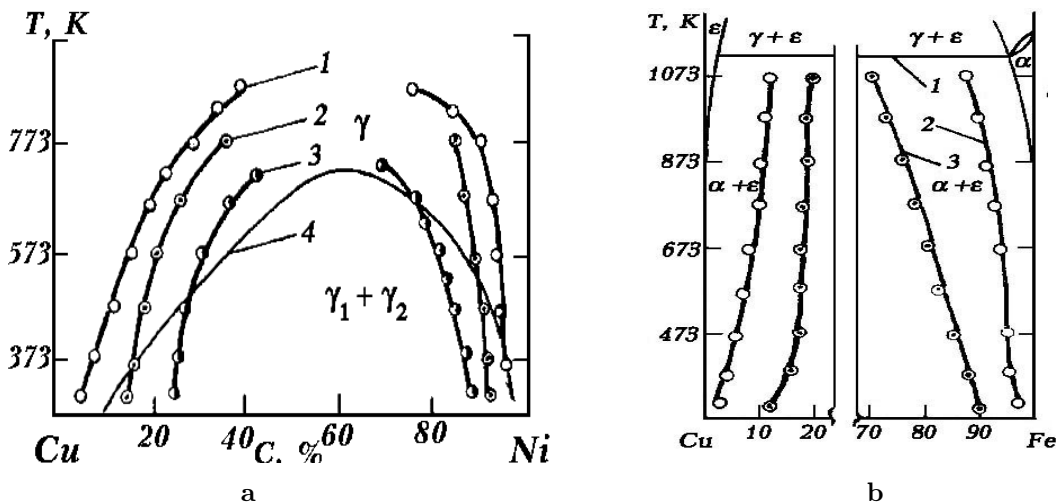


Fig. 2. Fragments of phase diagrams for Cu-Ni (a,1) and Cu-Fe (b,1) systems and the temperature dependences of the component concentrations in solid solutions at  $\dot{\epsilon} = 1$  (a,1), 10 (a,2), and 100  $s^{-1}$  (a,3) and  $\dot{\epsilon} = 5$  (b,2) and 200  $s^{-1}$  (b,3)

atoms at different time moments). The frequency of front-induced additional jumps of an interstitial defect does not depend on the temperature. It is governed by the wave front velocity, so that the latter can be regarded as one of the factors that stimulate ballistic jumps.

### 3. Modified Version of Martin's Kinetic Model

The physical problem under consideration has two aspects: thermodynamic and kinetic ones. The former consists in that the usual thermodynamic stimuli of diffusion transformations, as follows from the results of the described experiments, do not work, if the system is dynamically affected. It manifests itself in the formation of nonequilibrium states – supersaturated solid solutions – in the diffusion region (Fig. 2). The latter is related to the mechanisms of realization of those nonequilibrium states, being a limiting factor owing to a finite rate of diffusion relaxation. Since the pulse impact on the specimen is rather short in time, the final nonequilibrium state, which should have appeared due to the external dynamic influence, has no time to be realized during the experiment. This means that the experimental curves given in Fig. 2 can be considered only as such that describe the tendency of dynamic equilibrium to shift toward supersaturation, rather than the dynamic state diagrams. We do not deal with diffusion kinetics in this work. Therefore, the issue to what extent the experimental curves approach stationary states under the pulse impact remains beyond the scope of consideration. Instead, we will examine the

problem of the construction of dynamic state diagrams for a binary single-crystalline system  $A-B$ , which has a decomposition dome under equilibrium conditions. The thermodynamic characteristics of the alloy are determined by the energies of pair interaction between atoms,  $E_{AA}$ ,  $E_{BB}$ , and  $E_{AB}$  which are to be fitted to provide a wide enough spinodal region.

In order to explain the concentration shift in the decomposition dome of a dynamic state diagram, we considered the model of atomic migration. In the simplest case, we chose the kinetic model proposed by Martin for one-dimensional diffusion by the exchange mechanism [11]. This model is used to analyze diffusion in a binary alloy with an fcc lattice along the direction normal to the family of  $\{111\}$  planes. The basic equations of the model are as follows. For the concentration change of component  $B$  in the  $n$ -th plane, we have

$$\dot{c}_n = J_{n-1 \rightarrow n} - J_{n \rightarrow n+1},$$

$$J_{n \rightarrow n+1} = z [c_n(1 - c_{n+1})\Gamma_{n \rightarrow n+1} - c_{n+1}(1 - c_n)\Gamma_{n+1 \rightarrow n}], \tag{2}$$

where  $J_{n \rightarrow n+1}$  is the flux density of atoms  $B$  from plane  $n$  to plane  $n + 1$ ,  $z$  the number of nearest neighbors in adjacent planes ( $z = 3$ ),

$$\Gamma_{n \rightarrow n+1} = \nu \exp\left(-\frac{E_{n \rightarrow n+1}}{kT}\right) \tag{3}$$

is the frequency of the exchange between atom  $B$  from plane  $n$  and atom  $A$  from plane  $n + 1$ , and  $E_{n \rightarrow n+1}$  the

corresponding activation barrier which can be found as

$$E_{n \rightarrow n+1} = E_o + (E_{AB} - E_{BB})(z c_{n-1} + z c_{n+1} + z_o c_n) + (E_{AA} - E_{AB})(z c_n + z c_{n+2} + z_o c_{n+1}), \quad (4a)$$

$$E_{n+1 \rightarrow n} = E_o + (E_{AB} - E_{BB})(z c_n + z c_{n+2} + z_o c_{n+1}) + (E_{AA} - E_{AB})(z c_{n-1} + z c_{n+1} + z_o c_n). \quad (4b)$$

$z_0$  is the number of nearest neighbors in the same plane ( $z_0 = 6$ ), and  $E_0$  the constant energy in a saddle-point configuration under the  $A - B$  exchange.

To obtain the equilibrium phase diagram, we solved the diffusion problem (2). In so doing, the stationary diffusion profile was calculated using an explicit scheme and substitutions (3) and (4). As initial conditions, a step-like concentration distribution

$$c_n = \begin{cases} c_l, & n < 0, \\ (c_l + c_r)/2, & n = 0, \\ c_r, & n > 0 \end{cases}$$

was selected. Here,  $-N \leq n \leq N$ ,  $N$  was varied from 10 to 30, and  $c_l < 0.5 < c_r$ . The boundary conditions of the second kind with zero diffusion currents were specified at both boundaries:  $c_{-N} = c_{-N+1} = c_{-N+2}$  and  $c_N = c_{N-1} = c_{N-2}$ . It was found that the stationary profile does not depend on the initial values of  $c_l$  and  $c_r$ , and the equilibrium concentrations do not depend on the spatial extension of a specimen along the diffusion direction, if  $N \geq 10$ . (This is also true for next two sections, where other diffusion mechanisms are considered.) As the equilibrium concentrations, we naturally took the stationary values  $c_{-N}$  and  $c_N$ . The result of such a calculation is depicted in Fig. 3.

Now, let us consider the contribution of ballistic jumps according to Eq. (1). Since we have the exchange mechanism of diffusion, the ballistic term  $b$  cannot be treated as a contribution of induced jumps of defect. Instead, we assume that the pulse impact on the specimen gives rise to an effective reduction of activation barrier for some sites:

$$\Gamma_{n \rightarrow n+1} = \nu \left\{ \exp \left( -\frac{E_{n \rightarrow n+1}}{kT} \right) + b \right\}, \quad (5)$$

$$b = K \exp \left( -\frac{E}{kT} \right),$$

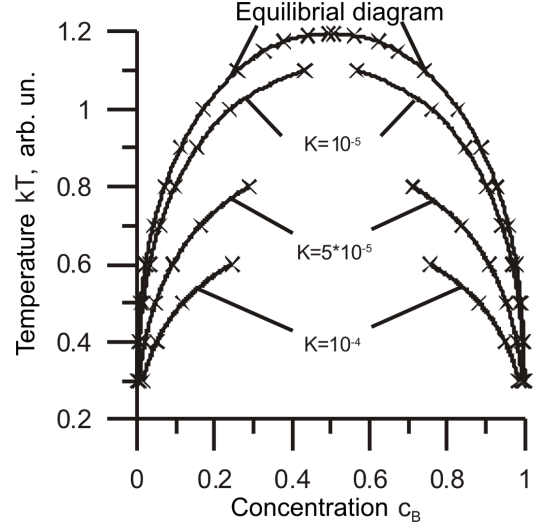


Fig. 3. Dynamic phase diagrams for Martin's model.  $E_{AA} = E_{BB} = -1.2$  and  $E_{AB} = -1.0$

where  $K$  is associated with a fraction of “ballistically activated” sites, which can be proportional to  $\varepsilon^2$  [12], and  $E$  is a reduced (in comparison with  $E_{n \rightarrow n+1}$ ) activation barrier.

The results of numerical calculations of dynamic phase diagrams, where Eq. (5) was used for various  $K$ -values and a simplified assumption  $E = E_0$  was made, are shown in Fig. 3. Hereafter, all energy characteristics are expressed in units of  $kT_0$ , where  $T_0$  is a certain initial temperature. For all other temperature values, the dimensionless quantity  $T/T_0$  is used. Figure 3 illustrates a rather good qualitative agreement with experimental data; in particular, as the ballistic term associated with the plastic deformation rate increases, the supersaturation of solid solutions grows, and it is just the behavior that the curves of dynamic phase diagrams demonstrate.

#### 4. The Mechanism of Interstitial Migration

The results discussed above were obtained in the framework of a rather simple but nonrealistic diffusion model of direct exchanges. Provided a pulse loading, more probable is the interstitial mechanism of “kick-out” diffusion [1]. Consider a bcc lattice (Fig. 4). It is enough to confine the consideration to octahedral interstitial positions only (designated by squares and crosses). The following assumptions concerning elementary diffusion events are made: (i) “kick-out” is a unique mechanism of diffusion, (ii) every interstitial atom can supersede only the nearest site neighbor (for crosses in Fig. 4, it is one

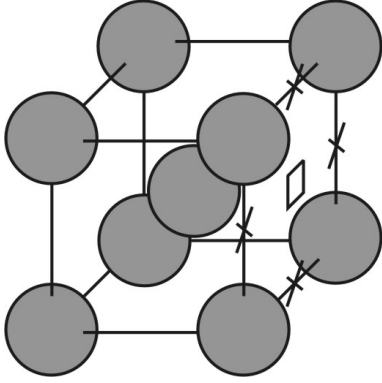


Fig. 4. Elementary bcc cell with designated interstitials

of cube's vertices; for the square, it is the interstitial site), (iii) a knocked out atom moves into the nearest interstitial site opposite with respect to the knocking-out atom (for instance, the internal atom in Fig. 4, being shifted from the square, moves to the opposite face, whereas any of the vortex atoms moves from a cross along one of the cube's edges into the next cubic cell, remaining in the vertical plane at that), (iv) possible direct jumps of interstitials from a "cross" position into a "square" one and *vice versa*.

Consider the one-dimensional diffusion in a binary alloy along the direction normal to (100) planes. Let  $c_n$ ,  $c_n^A$ , and  $c_n^B$  denote the concentrations of component  $B$  at lattice sites and interstitial sites  $A$  and  $B$  in the  $n$ -th plane, respectively. The kinetic equation is constructed taking the law of conservation into account. Simple, but laborious computations bring about the expressions

$$\begin{aligned} \frac{dc_n}{dt} = & -c_n \frac{c_{n+1}^A}{\nu} \Gamma_{n+1 \rightarrow n}^{AB} - c_n \frac{c_{n-1}^A}{\nu} \Gamma_{n-1 \rightarrow n}^{AB} - \\ & -c_n \frac{z_0 c_n^A}{\nu} \Gamma_{n \rightarrow n}^{AB} + (1 - c_n) \frac{c_{n+1}^B}{\nu} \Gamma_{n+1 \rightarrow n}^{BA} + \\ & + (1 - c_n) \frac{c_{n-1}^B}{\nu} \Gamma_{n-1 \rightarrow n}^{BA} + (1 - c_n) \frac{z_0 c_n^B}{\nu} \Gamma_{n \rightarrow n}^{BA}, \quad (6) \\ \frac{dc_n^A}{dt} = & -\frac{c_n^A}{\nu} c_{n+1} \Gamma_{n \rightarrow n+1}^{AB} - \frac{c_n^A}{\nu} (1 - c_{n+1}) \Gamma_{n \rightarrow n+1}^{AA} - \\ & -\frac{c_n^A}{\nu} c_{n-1} \Gamma_{n \rightarrow n-1}^{AB} - \frac{c_n^A}{\nu} (1 - c_{n-1}) \Gamma_{n \rightarrow n-1}^{AA} - \\ & -\frac{c_n^A}{\nu} z_0 c_n \Gamma_{n \rightarrow n}^{AB} - \frac{2c_n^A}{\nu} \Gamma_{n \rightarrow n+1}^{\prime A} - \end{aligned}$$

$$\begin{aligned} & -\frac{2c_n^A}{\nu} \Gamma_{n \rightarrow n-1}^{\prime A} + (1 - c_{n+1}) \frac{c_{n+2}^A}{\nu} \Gamma_{n+2 \rightarrow n+1}^{AA} + \\ & + (1 - c_{n+1}) \frac{c_{n+2}^B}{\nu} \Gamma_{n+2 \rightarrow n+1}^{BA} + (1 - c_{n-1}) \frac{c_{n-2}^A}{\nu} \Gamma_{n-2 \rightarrow n-1}^{AA} + \\ & + (1 - c_{n-1}) \frac{c_{n-2}^B}{\nu} \Gamma_{n-2 \rightarrow n-1}^{BA} + \frac{c_n^B}{\nu} z_0 (1 - c_n) \Gamma_{n \rightarrow n}^{BA} + \\ & + \frac{2c_{n+1}^A}{\nu} \Gamma_{n+1 \rightarrow n}^{\prime A} + \frac{2c_{n-1}^A}{\nu} \Gamma_{n-1 \rightarrow n}^{\prime A} \quad (7) \end{aligned}$$

and an analogous equation for  $c_n^B$  with the substitutions  $A \leftrightarrow B$  and  $c_i \leftrightarrow (1 - c_i)$ . Here,  $\nu$  is the number of interstitial sites per site atom ( $\nu = 3$ , see Fig. 4),  $z_0$  the number of nearest interstitial sites in the same plane ( $z_0 = 4$ ),  $\Gamma_{i \rightarrow j}^{XY}$  the displacement frequency of atom  $Y$  in the  $j$ -th plane by an interstitial atom of kind  $X$  from the  $i$ -th plane, and  $\Gamma_{i \rightarrow j}^{\prime X}$  the frequency of jumps by interstitial atom  $X$  from the  $i$ -th into the  $j$ -th plane. Taking the nonequilibrium conditions at the pulse action into consideration, those frequencies are expressed in terms of the corresponding activation barriers and ballistic terms as follows:

$$\begin{aligned} \Gamma_{i \rightarrow j}^{XY} = & \nu_o \exp \left( -\frac{E_{i \rightarrow j}^{XY}}{kT} \right) + b, \\ \Gamma_{i \rightarrow j}^{\prime X} = & \nu'_o \exp \left( -\frac{E'_{i \rightarrow j}^X}{kT} \right) + b, \quad (8) \end{aligned}$$

where  $b$  is a constant depending on the deformation rate. For the activation barrier, we have

$$E_{i \rightarrow j}^{XY} = E_o - E_j^Y - E_i^X, \quad E'_{i \rightarrow j}^X = E'_o - E_i^X, \quad (9)$$

where  $E_o$  and  $E'_o$  are saddle-point energies for "kick-out" events and direct interstitial hoppings, respectively (they are considered to be constant again);  $E_j^Y$  is the energy of component  $Y$  at the site; and  $E_i^X$  the energy of component  $X$  at the interstitial site:

$$\begin{aligned} E_j^Y = & 4(c_{j-1} + c_{j+1})E_{YB} + 4(2 - c_{j-1} - c_{j+1})E_{YA}, \\ E_i^X = & c_i E'_{XB} + (1 - c_i) E'_{XA}. \quad (10) \end{aligned}$$

To prevent extra complications associated with boundary conditions for interstitial sites and to solve the system of equations (6), (7) with substitutions (8) to (10), we impose periodic boundary conditions (a multilayer) which are algorithmically realized by virtually identifying the plane numbers:  $(N + i) \equiv (-N + i - 1)$  and  $(-N - i) \equiv (N - i + 1)$  at  $i = 1, 2$ . The stationary concentration profile was calculated for initial component concentration profiles  $c_n$  analogous to those in the case of exchange diffusion and provided that the initial distributions of interstitial atoms were uniform:  $c_n^A = c_n^B = \text{const.}$  We specially verified that the total initial number of interstitial atoms did not affect the final diffusion profile, but determined the rate of its establishment only; therefore, to speed up calculations, this quantity was set a little overestimated ( $\text{const} = 10^{-4} \div 10^{-3}$ ). The stationary values of  $c_{[-N/2]}$  and  $c_{[N/2]}$  at  $N = 10 \div 30$ , where [...] means the integer part of a number, were taken as equilibrium concentrations. The results of calculations are exhibited in Fig. 5. The supersaturation grows with increase in the ballistic frequency.

## 5. The Mechanism of Vacancy Diffusion

The basic importance of interstitial migration, which has been considered above, is determined by the dominant role of this diffusion mechanism at anomalous mass transfer in the course of pulse impact (as has already been pointed out earlier). But, when explaining the formation of alloys with a nonequilibrium composition in the diffusion region, this mechanism does not cover all possibilities. Really, in the framework of the ballistic jump concept, a similar effect should be expected for practically every activation process, as we have already demonstrated for the cases of exchange and interstitial diffusion. It is quite probable that the supersaturation process is implemented simultaneously through several channels under a pulse loading, and it is very probable that one of the key mechanisms of its realization is vacancy diffusion. Therefore, we intend to develop this model and to study it as well.

Like two previous cases, consider the one-dimensional diffusion in a two-component alloy with vacancies (a three-component system  $A-B-V$ ) in the direction normal to a certain family of crystal planes. The probability of the exchange between atom  $X$  in the  $n$ -th plane with a vacancy belonging to its first coordination sphere in the next  $m$ -th plane ( $m = n \pm 1$ ) per time unit is evidently equal to  $c_n^X p_m^{V,X} \Gamma_{n \rightarrow m}^X$ , where

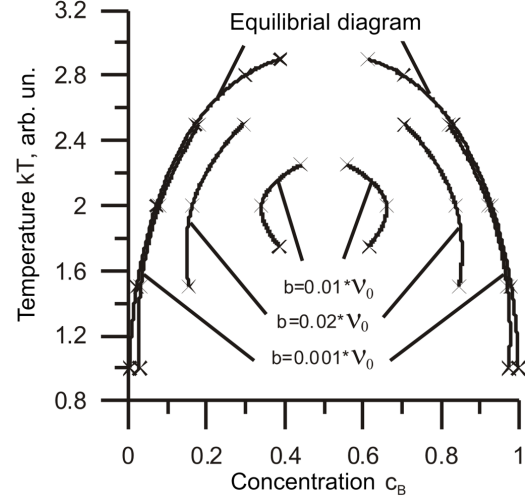


Fig. 5. Dynamic phase diagrams for the interstitial migration model.  $E_{AA} = E_{BB} = -1.75$ ,  $E_{AB} = -1.0$ ,  $E'_{AA} = E'_{BB} = E'_{AB} = -0.1$ , and  $\nu'_0 = 2\nu_0$

$c_n^X$  is the concentration of atoms in the  $n$ -th plane,  $p_m^{V,X}$  the probability that a vacancy and atom  $X$  meet in the  $m$ -th plane, and  $\Gamma_{n \rightarrow m}^X$  the frequency of the corresponding exchanges between such an atom and a vacancy. Then, for the variation rates of atomic and vacancy concentrations in the  $n$ -th plane, we can write down

$$\frac{1}{z} \frac{dc_n^X}{dt} = -c_n^X p_{n+1}^{V,X} \Gamma_{n \rightarrow n+1}^X - c_n^X p_{n-1}^{V,X} \Gamma_{n \rightarrow n-1}^X + c_{n+1}^X p_n^{V,X} \Gamma_{n+1 \rightarrow n}^X + c_{n-1}^X p_n^{V,X} \Gamma_{n-1 \rightarrow n}^X, \quad (11)$$

$$\begin{aligned} \frac{1}{z} \frac{dc_n^V}{dt} = & -p_n^{V,B} c_{n+1}^B \Gamma_{n+1 \rightarrow n}^B - p_n^{V,A} c_{n+1}^A \Gamma_{n+1 \rightarrow n}^A - \\ & - p_n^{V,B} c_{n-1}^B \Gamma_{n-1 \rightarrow n}^B - p_n^{V,A} c_{n-1}^A \Gamma_{n-1 \rightarrow n}^A + \\ & + p_{n+1}^{V,B} c_n^B \Gamma_{n \rightarrow n+1}^B + p_{n+1}^{V,A} c_n^A \Gamma_{n \rightarrow n+1}^A + \\ & + p_{n-1}^{V,B} c_n^B \Gamma_{n \rightarrow n-1}^B + p_{n-1}^{V,A} c_n^A \Gamma_{n \rightarrow n-1}^A, \end{aligned} \quad (12)$$

where  $z$  is the number of nearest neighbors of the lattice site in the next plane. The component concentrations are connected by the obvious relation

$$c_n^A + c_n^B + c_n^V = 1, \quad (13)$$

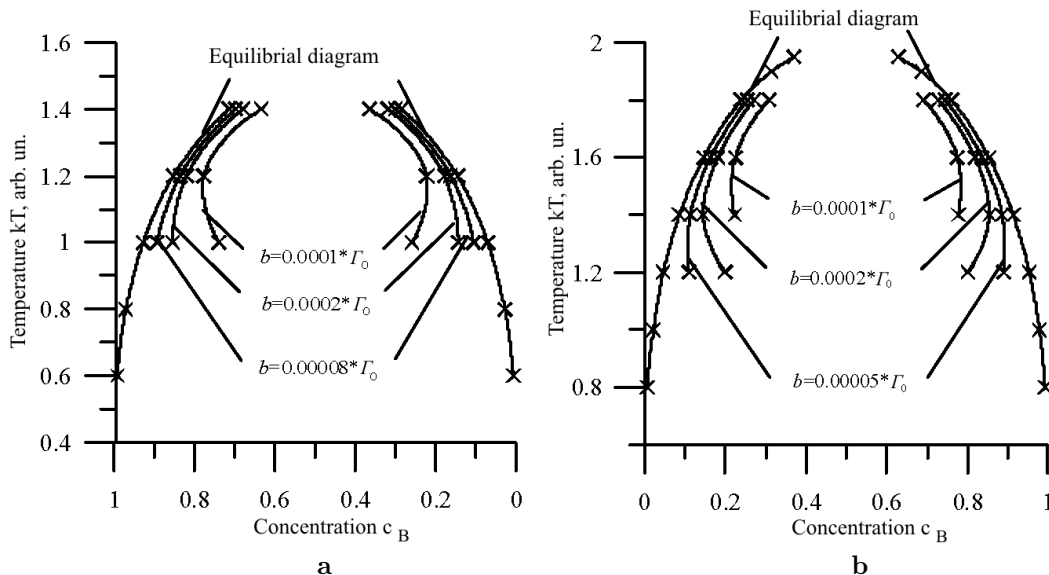


Fig. 6. Dynamic phase diagrams for the vacancy diffusion model in a simple cubic (a) and a bcc (b) lattice.  $E_{AA} = E_{BB} = -1.5$  and  $E_{AB} = -1.0$

which enables us to consider only one example of Eq. (11), for example, for atoms  $B$ .

The probabilities of meetings with a vacancy are determined from the standard Boltzmann distribution:

$$\frac{p_n^{V,X}}{c_n^V} = \frac{\exp(-E_n^{V,X}/kT)}{\exp(-\bar{E}_n^V/kT)},$$

where  $c_n^V$  is the vacancy concentration in the  $n$ -th plane,  $\bar{E}_n^V$  the average vacancy energy in the same plane, and  $E_n^{V,X}$  the *a posteriori* energy of a vacancy in the  $n$ -th plane, provided that atom  $X$  is its neighbor. Hence,

$$p_n^{V,X} = c_n^V \exp\left(\frac{\bar{E}_n^V - E_n^{V,X}}{kT}\right). \quad (14)$$

Let us express those energies in terms of pair binding energies of atoms in the mean-field approximation and without taking a small difference between component concentrations in next planes into account:

$$\bar{E}_n^V = -Z(2c_n^A c_n^B E_{AB} + (c_n^A)^2 E_{AA} + (c_n^B)^2 E_{BB}), \quad (15)$$

$$E_n^{V,X} = -(Z-1)(2c_n^A c_n^B E_{AB} + (c_n^A)^2 E_{AA} + (c_n^B)^2 E_{BB}) - (c_n^X E_{AB} + c_n^X E_{XX}), \quad (16)$$

where  $Z$  is the coordination number.

The expression for the frequencies of vacancy exchanges, which takes the ballistic term  $b$  associated with the plastic deformation rate into account, reads

$$\Gamma_{n \rightarrow m}^X = \Gamma_0 \exp\left(-\frac{E_{n \rightarrow m}^X}{kT}\right) + b, \quad (17)$$

where, as usual,  $\Gamma_0$  is a constant frequency factor, and  $E_{n \rightarrow m}^X$  the activation barrier for the jump of atom  $X$  from the  $n$ -th plane into a vacant site in the  $m$ -th one. Again, if we suggest that the saddle configuration level is identical for every jump and choose it as the reference point on the energy scale, the following expression for the barrier is obtained (neglecting also the concentration gradients):

$$E_{n \rightarrow m}^X = -(Z-1)(c_n^X E_{AB} + c_n^X E_{XX}), \quad (18)$$

where the lack of an interatomic bond due to a neighbor vacancy is taken into account (the energy of interaction with the vacancy is taken equal to zero).

As was done earlier, in order to calculate the equilibrium and nonequilibrium state diagrams, we have to obtain the stationary solution of the system of equations (11), (12), making allowance for condition (13) and substitutions (14) to (18). This problem for the diffusion between planes of the (100) family in simple cubic ( $Z = 6$  and  $z = 1$ ) and bcc ( $Z = 8$  and  $z = 4$ ) lattices with periodic boundary conditions was solved numerically. Again, as was in the case of interstitial

migration, the result does not depend on the initial number of vacancies, the latter quantity affecting only the rate of stationary distribution establishment. The initial vacancy concentration was set uniform over the whole specimen volume, ranging from 0.01 to 0.1%. The results of calculations are depicted in Fig. 6. Note again the correspondence between our numerical model and experimental data: the growth of the ballistic term (the growth of the deformation rate) is accompanied by an increase of supersaturation in solid solutions.

## 6. Conclusions

We have theoretically analyzed the phenomenon of the formation of supersaturated solid solutions in the diffusion region between two metal components subjected to a pulse loading and undergoing a plastic deformation. The results of experimental researches revealed the dependence of the supersaturation on the deformation rate. We managed to explain this effect on the basis of microscopic models of diffusion involving the mechanisms of direct exchanges and migration of point defects in crystals with ballistically induced events (in contrast and in addition to thermally activated events). All the examined models turned out to produce plausible nonequilibrium phase diagrams with the supersaturation typical of relevant experiments. This allows us to suggest that this effect is characteristic of the activation processes in general, irrespective of a specific diffusion mechanism. From this viewpoint, the interstitial and vacancy mechanisms are identically efficient, provided the corresponding non-thermal (ballistic) contribution, and can be responsible for the observed phenomenon of supersaturation in solid solutions at a pulse loading.

The work was partially supported by the State Fund for Fundamental Researches of Ukraine (project No. F25.4/162 and contract No. f25/571-2007 "Phase formation under conditions of shock loading and electric current").

1. V.F. Mazanko, A.V. Pokoev, V.M. Mironov *et al.*, *Diffusion Processes in Metals Under the Action of Magnetic Fields and Pulse Deformations, Vols. 1 and 2* (Mashinostroenie, Moscow, 2006) (in Russian).
2. A.I. Ignatenko and G.K. Kharchenko, *USSR invention certificate No. 404508*, Int. Cl. B23K 20/00, published 14.12.73.
3. D.S. Gertsriken, V.F. Mazanko, A.I. Ignatenko, G.K. Kharchenko, and O.A. Mironova, *Fiz. Met. Metalloved.* **99**, 187 (2005).
4. D.S. Gertsriken, V.F. Mazanko, O.A. Mironova, L.A. Mitlina, and O.I. Nosovskii, *Dopov. Nat. Akad. Nauk Ukr.*, N 8, 119 (2006).
5. V.M. Mironov, O.A. Mironova, D.S. Gertsriken, V.F. Mazanko, and L.A. Mitlina, *Probl. Mashinostr. Avotmat.*, N 2, 71 (2005).
6. V.M. Mironov, O.A. Mironova, L.A. Mitlina, D.S. Gertsriken, and A.I. Ignatenko, *Fiz. Khim. Obrab. Mater.*, N 4, 77 (2006).
7. D.S. Gertzriken, T.V. Kolenova, and A.M. Gusak, *Defect Diff. Forum* **194-199**, 1469 (2000).
8. A.M. Gusak *et al.*, *Models of Solid-Phase Reactions* (Cherkasy Nat. Univ. Publ. House, Cherkasy, 2004) (in Russian).
9. G. Martin, *Phys. Rev. B* **30**, 1424 (1984).
10. J.B. Gibson, A.N. Goland, M. Milgram, and G.H. Vineyard, *Phys. Rev.* **120**, 1229 (1960).
11. G. Martin, *Phys. Rev. B* **41**, 2279 (1990).
12. A.O. Koval'chuk, D.S. Gertzriken, A.M. Gusak, V.F. Mazanko, *Defect Diff. Forum* **277**, 69 (2008).

Received 09.01.08.

Translated from Ukrainian by O.I. Voitenko

## МОДЕЛІ ОТРИМАННЯ СПЛАВІВ НЕРІВНОВАЖНОГО СКЛАДУ В ОБЛАСТІ ДИФУЗІЙНОГО КОНТАКТУ ДВОХ КОМПОНЕНТІВ ПІД ДІЄЮ ІМПУЛЬСНИХ НАВАНТАЖЕНЬ

A.O. Ковальчук, Д.С. Герцрікен, А.М. Гусак, В.Ф. Мазанко, Н.В. Тютюнник, О.І. Малій

### Резюме

В експериментах з дослідження дифузії у металах і сплавах під дією імпульсних навантажень досить часто спостерігається формування метастабільних сплавів із межами розчинності, що набагато перевищують рівноважні значення й залежать від швидкості деформації. Для теоретичного опису формування у дифузійній парі метастабільних твердих розчинів під час імпульсного навантаження було запропоновано три мікроскопічні моделі, що ґрунтуються на концепції "балістичних стрибків" (запропонованій Мартеном із співавторами для матеріалів під дією опромінення або при механічному перемішуванні): 1) модель обмінної дифузії; 2) модель міжвузловинної міграції та 3) вакансійну модель дифузії. У рамках усіх цих трьох моделей було отримано динамічні фазові діаграми та зіставлені з отриманими раніше експериментальними даними. Було отримано якісне збігання результатів.